

## Streak camera imaging of single photons at telecom wavelength

Markus Allgaier,<sup>1</sup> Vahid Ansari,<sup>1</sup> Christof Eigner,<sup>1</sup> Viktor Quiring,<sup>1</sup> Raimund Ricken,<sup>1</sup> John Matthew Donohue,<sup>1</sup> Thomas Czerniuk,<sup>2</sup> Marc Aßmann,<sup>2</sup> Manfred Bayer,<sup>2</sup> Benjamin Brecht,<sup>1,3</sup> and Christine Silberhorn<sup>1</sup>

<sup>1</sup>*Integrated Quantum Optics, Applied Physics, University of Paderborn, 33098 Paderborn, Germany*

<sup>2</sup>*Experimentelle Physik II, Technische Universität Dortmund, D-44221 Dortmund, Germany*

<sup>3</sup>*Clarendon Laboratory, Department of Physics, University of Oxford, Oxford OX1 3PU, United Kingdom*

(Received 11 September 2017; accepted 5 January 2018; published online 19 January 2018)

Streak cameras are powerful tools for temporal characterization of ultrafast light pulses, even at the single-photon level. However, the low signal-to-noise ratio in the infrared range prevents measurements on weak light sources in the telecom regime. We present an approach to circumvent this problem, utilizing an up-conversion process in periodically poled waveguides in Lithium Niobate. We convert single photons from a parametric down-conversion source in order to reach the point of maximum detection efficiency of commercially available streak cameras. We explore phase-matching configurations to apply the up-conversion scheme in real-world applications. *Published by AIP Publishing.* <https://doi.org/10.1063/1.5004110>

Characterization of ultrafast pulses with pulse durations of only a few picoseconds or less is a challenge, especially when it comes to the direct observation in the time domain. Optical autocorrelation measurements<sup>1,2</sup> and streak cameras<sup>3</sup> are among the most popular techniques to measure the temporal intensity envelope of photons. Indirect temporal measurements using spectral shearing interferometry,<sup>4,5</sup> also known as SPIDER, and frequency resolved optical gating,<sup>6</sup> known as FROG, have been demonstrated, where time-domain information can be extracted through the Fourier transform. Streak cameras are able to provide *direct* temporal measurements at the single-photon level<sup>7–9</sup> and have become standard tools in semiconductor physics. Streak cameras allow for the measurement of many different degrees of freedom,<sup>10,11</sup> and one reason for the device's success is the possibility to record time-resolved spectra in combination with a spectrometer. However, streak cameras rely on the conversion of light to electrons using photocathodes, which are generally inefficient at wavelengths longer than 900 nm. In fact, all demonstrations of streak camera measurements at a single-photon level have been performed at wavelengths shorter than 900 nm. No matter whether the light source was a semiconductor system,<sup>9,12–14</sup> parametric down-conversion source<sup>15</sup> or organic molecules,<sup>16</sup> the emission was in the spectral range where streak cameras operate at high quantum efficiency. While single-photon-level operation is possible in the visible and near-infrared range, to date, there is no commercial streak camera system capable of detecting *telecom* light at the single-photon level with satisfactory quantum efficiency. As streak cameras are known to be powerful tools for low-light applications, such tools for infrared light would certainly prove tremendously useful.

Using an atomic gas chamber instead of a classical photocathode improves infrared sensitivity over a broad spectral range<sup>17</sup> but highlights that further development of telecom-sensitive streak cameras is technically very challenging. Already early in the development of streak cameras, this issue was circumvented using an up-conversion detection

system<sup>18</sup> based on a sum-frequency generation (SFG) process, but this implementation suffered from low detection efficiency, limited by the conversion efficiency of the SFG. The scheme was used later on to detect high intensity radiation from a CO<sub>2</sub> laser.<sup>19</sup> The up-conversion streak camera was superseded when models with different cathode materials made the direct observation of infrared light in the telecom band possible<sup>20</sup> but still with highly limited efficiency.

Since the development of the up-conversion streak camera, there have been experiments showing the value of up-conversion techniques for single-photon measurements. Besides up-conversion assisted photon counting,<sup>21</sup> direct temporal measurements using up-conversion have been demonstrated. One example is the measurement of the temporal intensity of photons from a parametric down-conversion (PDC) source.<sup>22,23</sup> However, this method cannot provide a simultaneous observation of two degrees of freedom such as time and frequency, as would be possible with a streak camera when combined with a spectrometer. However, only a very high-efficiency conversion process can enable single-photon detection beyond 900 nm with a streak camera.

Pulsed PDC sources are ideal candidates for verifying the performance of any measurement apparatus at the single-photon level. Indeed, it has been suggested to use PDC sources for detector calibration.<sup>24</sup> The mean photon number can be readily ascertained from only the click- and coincidence rates, for example, using an avalanche photodiode. The mean photon number of the light source under investigation, in particular, is a parameter not often found in the streak camera-related literature, despite being essential for the evaluation of the performance of streak cameras at the single-photon level.

In this letter, we demonstrate that the detection of single photons in the infrared range at a wavelength of 1550 nm is possible when a highly efficient up-conversion process is employed. We propose to use a conversion process that stretches the pulse in order to increase the temporal resolution. The concept of pulse stretching while keeping the time-bandwidth-product constant, i.e., bandwidth compression,

has been demonstrated using SFG;<sup>25</sup> however, the efficiency of the process needs to be significant to make observation using even the most sensitive streak cameras possible. We recently introduced a similar scheme that uses an engineered, waveguided SFG,<sup>26</sup> providing both a sufficient conversion efficiency and a bandwidth compression factor of 7.5. We demonstrate the performance of the up-conversion device together with a streak camera by measuring the temporal intensity envelope of single photons at wavelengths longer than 900 nm, namely, from a telecom PDC source.

The main noise source for streak cameras is thermionic emission from the photocathode.<sup>27</sup> At long wavelength, the detection of single photons is hindered by the strong cathode noise and low quantum efficiency. Cathode noise has been shown to add additional electrons during photo-electric conversion.<sup>28</sup> This makes direct observation of faint infrared signals beyond 900 nm highly difficult. Even though many streak camera models have electron multipliers that enable operation in a so-called “single-photon counting mode,” where a single photon causes an electron avalanche detectable on the phosphorus screen and CCD, this operation mode is unsuitable for infrared measurements since most of the amplified electrons arise from cathode noise. Moreover, it has been shown that drastic reduction of the repetition rate is required to achieve a better signal-to-noise ratio in the single-photon counting mode.<sup>9,29</sup> The dark count rate with a NaKSbCs-cathode (usually designated S-20) is in the range of 500 counts per second,<sup>30</sup> assuming a 5-mm cathode diameter. Even at 900 nm, the quantum efficiency of the mentioned cathode is as low as 0.1%<sup>27,31,32</sup> (and much lower at longer wavelengths), which implies that an input of 500 000 counts per second is required to achieve a signal-to-noise ratio of 1, not counting other noise sources like thermionic emission of other components, camera readout, and thermal noise. While the S-20 material is intended for use in the visible range, other cathode materials better suited for operation in the infrared range do exist, like InP/InGaAs or AgOCs (known as S-1). However, their quantum efficiency is of the same order of magnitude.<sup>27</sup> With the use of the presented up-conversion device, it is possible to harness the excellent quantum efficiency of S-20 photocathodes (40 mA/W@500 nm for S-20 vs. 1 mA/W for S-1<sup>31</sup>) for imaging of infrared radiation.

Figure 1 depicts the experimental apparatus. It consists of a photon pair source, a frequency converter, and a streak camera. The photon pairs are generated using a PDC source identical to the one used in Ref. 33. It provides photon pairs at a central wavelength of 1545 nm with a bandwidth of 6 nm. The source is pumped with pulses from a Ti:Sapphire laser with a pulse energy of 120 pJ, resulting in a moderately low mean photon number of 0.2 per pulse emitted by the source. The pump beam for the PDC source is generated by a cascade of an optical parametric oscillator (OPO) and second harmonic generation (SHG) in a periodically poled Lithium Niobate bulk crystal. We use a 4-f bandpass filter to narrow down the pump spectrum. The bandwidth is set to 3 nm, which yields a spectrally decorrelated PDC state.<sup>26</sup>

The photon pairs from the type-II process are separated with a polarizing beam splitter, and one of the photons is sent to the frequency converter. The conversion is achieved by means of a quantum pulse gate (QPG),<sup>34,35</sup> a device based

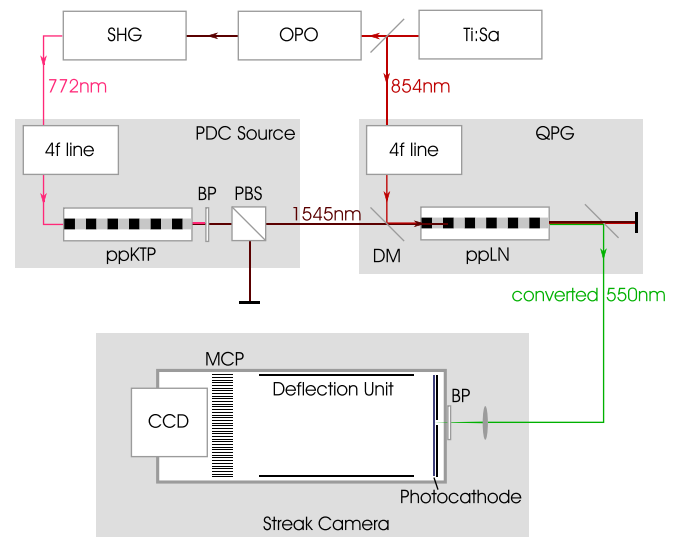


FIG. 1. Setup used in the experiment. Ti:Sa, titanium sapphire laser; OPO, optical parametric oscillator; SHG, second harmonic generation; BP, band pass filter; PBS, polarizing beam splitter; DM, dichroic mirror; SMF, single mode fiber; MCP, multi-channel plate; and CCD, charge coupled device; ppKTP, periodically poled Potassium Titanyl Phosphate; ppLN, periodically poled Lithium Niobate.

on a group-velocity matched SFG in Titanium-indiffused waveguides in Lithium Niobate. The process is pumped with pulses with a central wavelength of 854 nm from the Ti:Sapphire laser, shaped by a spatial light modulator (SLM) based pulse shaper. The pulse shaper allows us to shape the spectral intensity and phase to maximize the overlap with the PDC photons and therefore conversion efficiency. Using a 27-mm long crystal, we achieve an internal conversion efficiency of 61.5%. The details regarding the engineering, efficiency, and verification of group-velocity matching of the process are elaborated in Refs. 26 and 36.

We record the up-converted light at 550 nm on a Hamamatsu C5680 streak camera equipped with an S-1 photocathode and an ORCA-ER CCD camera. The device’s deflection circuit is being operated in the so-called synchroscan mode, where the deflection circuit’s repetition rate is synchronized and actively stabilized to the laser’s repetition rate of 80.165 MHz. The SFG process causes no additional constraints on the repetition rate. The photocathode is operated at room temperature. Its spectral response is 1 mA/W at 550 nm and below  $10^{-3}$  mA/W at 1550 nm.<sup>31</sup>

In Fig. 2, we show the resulting background-subtracted image captured with the streak camera’s CCD. The image is integrated over 32 individual exposures of 10 s each. While other camera models may permit longer exposures, this would merely reduce the impact of readout noise, while the dominant cathode noise persists. For the background image, the PDC beam path was blocked directly behind the source. The multi-channel plate gain was set to 2/3 of the maximum value. At larger amplification, the cathode noise became the dominating noise source. With these settings, the signal was just above the noise floor of the camera, where the readout noise dominated over the dark current. For this reason, the largest possible exposure time of ten seconds was chosen for this measurement. Fig. 3 shows the temporal intensity envelope extracted from Fig. 2 by integrating in the horizontal direction

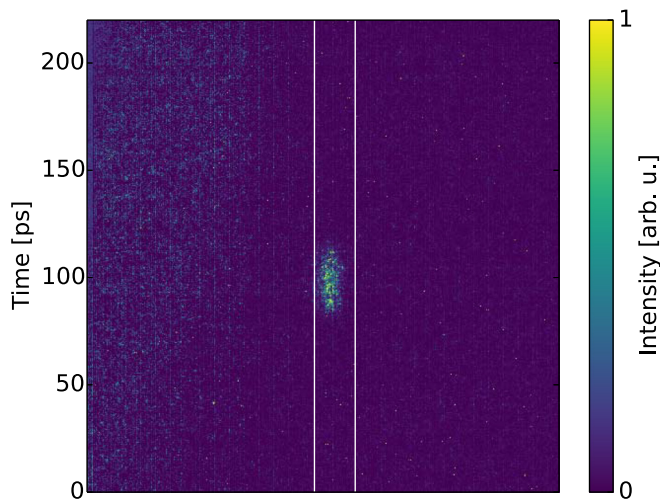


FIG. 2. Streak camera image for the up-converted PDC photon, obtained by analog integration over 32 exposures with a 10 s exposure time each. The white lines indicate the integration boundaries used to obtain the temporal profile. The horizontal axis covers merely the spatial degree of freedom and carries no physical information in this measurement scenario.

over the area bound by the white lines. Error bars were created from the fluctuations around the mean values inside 5 ps bins. This corresponds to the temporal resolution of the device as given by the focus spot size on the photocathode. Such an approach is reasonable as the imaged spot size on the CCD is much larger than the pixel size.

From previous measurements on the initial temporal intensity envelope in Ref. 23, the pulse duration before the conversion process is known to be  $1.1 \pm 0.2$  ps (FWHM). This up-conversion process alters the temporal envelope and stretches the pulse duration. From theory, we expect a duration of 27-ps with a long top-hat shape. The output is then convolved with the streak camera's response function given by its limited resolution of 5 ps. We therefore expect to measure a final pulse duration of 28.5 ps. However, the measured pulse duration is merely  $22.6 \pm 0.5$  ps. The initial photon pulse duration was confirmed using a non-linear cross-correlation technique.<sup>23</sup> Therefore, the observed discrepancy can only be

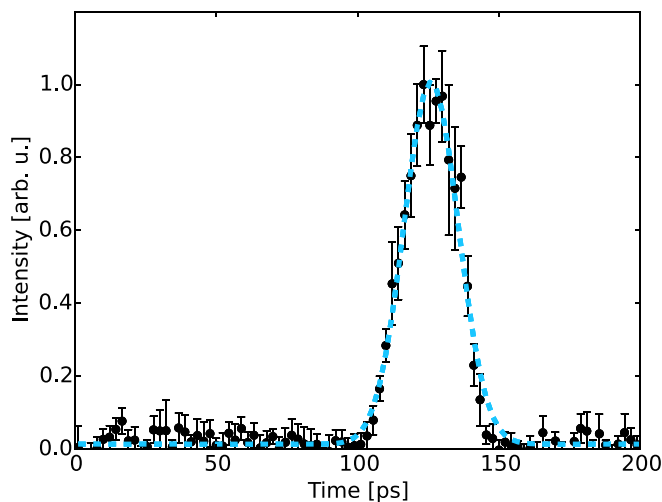


FIG. 3. Integrated temporal profile of the up-converted PDC photon obtained from the streak camera image in Fig. 2. Error bars were calculated using the standard deviation around the averaged counts in 5 ps bins. The blue dashed line indicates a Gaussian fit used to obtain the temporal duration.

caused by the conversion process. Imperfections in the periodic poling of the waveguide structure yield a shorter effective interaction length, resulting in a shorter output pulse. A shorter interaction length is in accordance with the asymmetric phase-matching measured in Ref. 26, as a perfectly homogeneous non-linearity profile over the whole crystal length would yield a symmetric sinc phase-matching spectrum, which is not observed in the sample employed here.

To ascertain how much the up-conversion scheme improves the overall detection efficiency, we must consider two key figures. First, the external conversion efficiency of the process, which includes how much light inside the waveguide is converted as well as linear losses, is measured to be 27.1%.<sup>26</sup> This linear loss is more than balanced out by the fact that the photocathode's quantum efficiency documented in the literature<sup>27,31,32</sup> is 3 orders of magnitude higher at 550 nm than it is at 1550 nm. The two numbers multiplied give rise to an improvement of the detection efficiency by a factor of at least 250. Other photocathode models exist that provide better quantum efficiency at 550 nm. These photocathodes have an efficiency enhanced by two orders of magnitude but may not be sensitive to telecom light at all. In terms of detection efficiency, our work conclusively shows that up-conversion schemes are viable to make single photons in the infrared range accessible by streak cameras. In this work, the brightness of the converted light was just barely above the detection limit of the streak camera; however, moving from the employed S-1 photocathode to the one that is more efficient at this wavelength would provide an improvement of 100 to the quantum efficiency.

The up-conversion process in combination with the particular streak camera used in this work facilitates the characterization of telecom photons. However, the configuration of the conversion, in particular, the engineered phase-matching, has both advantages and drawbacks. We define the phase-mismatch in a traditional way using the wavenumber  $k = 2\pi n(\lambda)/\lambda$ , where  $n$  denotes the effective refractive index of the waveguide mode and the poling period  $\Lambda$  used to achieve quasi-phase-matching

$$\Delta k = k_{\text{pump}} + k_{\text{input}} - k_{\text{output}} + \frac{2\pi}{\Lambda}. \quad (1)$$

This phase-matching function is the governing quantity of the up-conversion process. Its orientation with respect to the signal and idler frequency axes depends strongly on the dispersion  $\partial\omega/\partial k$  of the material and waveguide. In the process employed in this work, plotted in Fig. 4(a), the resulting spectral transfer function is flat, which means that the output is mostly independent of the input<sup>37</sup> and there are no spectral correlations between the two. On the one hand, this provides excellent conversion efficiency and bandwidth compression due to the group-velocity matching between input and the pump. However, the phase-matching of the process masks the temporal-spectral information of the PDC state. The calculated temporal amplitude  $s(t)$  of our process at the output of the waveguide reads<sup>38</sup>

$$s(t) \propto \int d\omega e^{j\omega t} \int d\omega_2 F_1(\omega - \omega_2) F_2(\omega_2) \times e^{-j\omega_2 \tau} e^{j(\Delta k + \alpha\omega)L/2} \times \text{sinc}\left(\left(\Delta k + \alpha\omega\right)\frac{L}{2}\right), \quad (2)$$

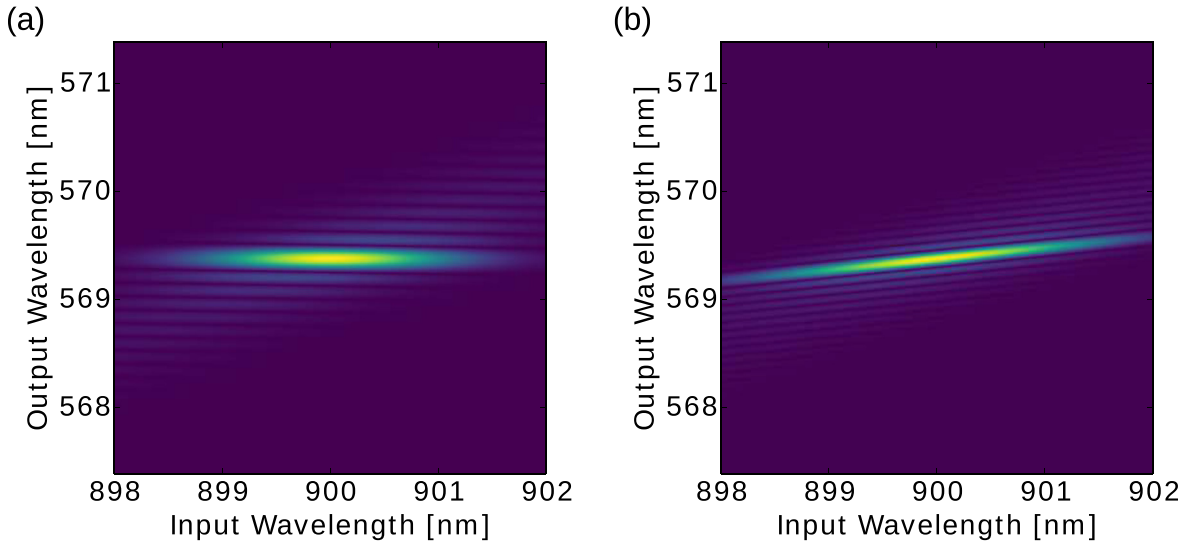


FIG. 4. (a) Spectral transfer function of the up-conversion process employed in this work. (b) Spectral transfer function of the proposed up-frequency generation process.

where  $\alpha = \dot{k}_s - \dot{k}_1$  denotes the mismatch between inverse group velocities of output and input,  $\Delta k$  again denotes the corresponding phase-mismatch,  $F_1(\omega)$  and  $F_2(\omega)$  are the spectral intensities of input and the pump with respect to angular frequencies, respectively, and  $L$  is the effective crystal length. First, the output is defined by a convolution of the pump and input spectra (see integral over  $\omega_2$ ). In our case, these have a comparable shape and bandwidth. Inside the Fourier transform (see integral over  $\omega$ ), this convolution is multiplied by a sinc-function which, in the case engineered here, only depends on the phase-mismatch and crystal length, as the group velocity mismatch  $\dot{k}_1 - \dot{k}_2$  is zero. The bandwidth of the photons in the experiment allows us to neglect dispersion. The temporal profile is therefore the Fourier transform of the convolved spectra of input and the pump, multiplied with the Fourier transform of the sinc-shaped phase-matching. In the temporal domain, the amplitude is therefore the convolution of individual Fourier transforms

$$s(t) = FT \left( \int d\omega_2 F_1(\omega - \omega_2) F_2(\omega_2) \right) * FT \left( \text{sinc} \left( (\Delta k + \alpha\omega) \frac{L}{2} \right) \right). \quad (3)$$

We find two competing timescales: One set by the duration of the input fields and the other by the crystal length. In our case, the temporal profile is dominated by the contribution of the sinc-function given by the long crystal. The Fourier transform of the spectral overlap integral, which has a duration of the order of 1 ps, is therefore convolved by a rectangular function of 27 ps width, which masks the temporal information about the PDC state significantly. While, in principle, the initial temporal profile could be reconstructed, faithful deconvolution may be highly dependent on the specific application, i.e., the crystal, streak-camera, and pulse shape used, imposing limits on the complexity of possible input pulse shapes.<sup>34,35</sup> While this has no impact on the improvement of the detection efficiency, a process which

preserves the temporal profile is desirable. It is therefore appropriate to consider alternative process conditions regarding group velocity matching and phase-matching.

In a general type-0 process, the transfer function [Fig. 4(b)] is angled compared to the one employed in this work [Fig. 4(a)]. The angle introduces correlations between input and output frequencies and therefore constitutes a means of direct mapping of pulse shapes in the limit where the input pulse bandwidth is much larger than the bandwidth of the transfer function. This facilitates a means of preserving the temporal envelope of the converted pulse. The temporal properties of such a process, e.g. pulse reversal and temporal stretching, have recently been investigated theoretically.<sup>39</sup> This type of process has already been employed in up-conversion detection schemes.<sup>21</sup> Since it makes use of the highest non-linear coefficient in Lithium Niobate, it can be highly efficient.

In the future, we hope to expand the scheme to heralded measurements, which would require some form of feed-forward beam blocking mechanism. While such fast pulse picking devices are lossy in general, the up-conversion approach presents the advantage that the SFG pump can be switched instead, hence providing lossless pulse picking. It is noteworthy that photon correlation measurements like the ones performed in Ref. 7 are still possible using up-conversion since the process has been shown to preserve non-classical photon number statistics.<sup>26</sup>

We demonstrated the feasibility of using a highly efficient SFG in Lithium Niobate to detect single photons at telecom wavelength on a streak camera. This allows to harness the exceptionally high quantum efficiency of photocathodes designed for use with visible radiation for imaging of infrared radiation. The exceptionally high efficiency of the process makes it feasible to employ streak cameras for various experiments in quantum optics not only as a means of direct temporal observation of single photons but also as a picosecond-resolution photon counter. For typical fluorescence spectroscopy applications, the up-conversion scheme could be used in a variety of ways, for example, the

characterization of the emission of infrared semiconductor laser structures far below threshold.

This work was funded by the Deutsche Forschungsgemeinschaft via SFB TRR 142 (C01) and via the Gottfried Wilhelm Leibniz-Preis.

- <sup>1</sup>J. A. Armstrong, *Appl. Phys. Lett.* **10**, 16 (1967).
- <sup>2</sup>V. Kabelka and A. V. Masalov, *Opt. Commun.* **121**, 141 (1995).
- <sup>3</sup>A. Campillo and S. Shapiro, *IEEE J. Quantum Electron.* **19**, 585 (1983).
- <sup>4</sup>D. N. Fittinghoff, I. A. Walmsley, J. L. Bowie, J. N. Sweetser, R. T. Jennings, M. A. Krumbügel, K. W. DeLong, and R. Trebino, *Opt. Lett.* **21**, 884 (1996).
- <sup>5</sup>A. O. Davis, M. Karpinski, and B. J. Smith, in *Conference on Lasers and Electro-Optics (2016)* (Optical Society of America, 2016), p. FTu4C.6.
- <sup>6</sup>D. J. Kane and R. Trebino, *IEEE J. Quantum Electron.* **29**, 571 (1993).
- <sup>7</sup>J. Wiersig, C. Gies, F. Jahnke, M. Aszmann, T. Berstermann, M. Bayer, C. Kistner, S. Reitzenstein, C. Schneider, S. Hoffing, A. Forchel, C. Kruse, J. Kalden, and D. Hommel, *Nature* **460**, 245 (2009).
- <sup>8</sup>M. Aßmann, F. Veit, M. Bayer, C. Gies, F. Jahnke, S. Reitzenstein, S. Höfling, L. Worschech, and A. Forchel, *Phys. Rev. B* **81**, 165314 (2010).
- <sup>9</sup>M. Aßmann, F. Veit, J.-S. Tempel, T. Berstermann, H. Stolz, M. van der Poel, J. M. Hvam, and M. Bayer, *Opt. Express* **18**, 20229 (2010).
- <sup>10</sup>R. Kodama, K. Okada, and Y. Kato, *Rev. Sci. Instrum.* **70**, 625 (1999).
- <sup>11</sup>L. Gao, J. Liang, C. Li, and L. V. Wang, *Nature* **516**, 74 (2014).
- <sup>12</sup>C. Santori, G. S. Solomon, M. Pelton, and Y. Yamamoto, *Phys. Rev. B* **65**, 073310 (2002).
- <sup>13</sup>H. Deng, G. Weihs, C. Santori, J. Bloch, and Y. Yamamoto, *Science* **298**, 199 (2002).
- <sup>14</sup>W. Langbein, *Phys. Rev. B* **70**, 205301 (2004).
- <sup>15</sup>R. Machulka, K. Lemr, O. Haderka, M. Lamperti, A. Allevi, and M. Bondani, *J. Phys. B: At., Mol. Opt. Phys.* **47**, 215501 (2014).
- <sup>16</sup>M. Komura and S. Itoh, *Photosyn. Res.* **101**, 119 (2009).
- <sup>17</sup>G. M. Lankhuijzen and L. D. Noordam, *Nucl. Instrum. Methods Phys. Res., Sect. A* **375**, 651 (1996).
- <sup>18</sup>N. Onodera, H. Ito, and H. Inaba, *Appl. Phys. Lett.* **43**, 720 (1983).
- <sup>19</sup>N. V. Pletnev, V. V. Apollonov, and V. R. Sorochenko, *Instrum. Exp. Tech.* **52**, 412 (2009).
- <sup>20</sup>I. H. White, D. F. G. Gallagher, M. Osinski, and D. Bowley, *Electron. Lett.* **21**, 197 (1985).
- <sup>21</sup>J. S. Pelc, L. Ma, C. R. Phillips, Q. Zhang, C. Langrock, O. Slattery, X. Tang, and M. M. Fejer, *Opt. Express* **19**, 21445 (2011).
- <sup>22</sup>O. Kuzucu, F. N. C. Wong, S. Kurimura, and S. Tovstonog, *Phys. Rev. Lett.* **101**, 153602 (2008).
- <sup>23</sup>M. Allgaier, G. Vigh, V. Ansari, C. Eigner, V. Quiring, R. Ricken, B. Brecht, and C. Silberhorn, *Quantum Sci. Technol.* **2**, 034012 (2017).
- <sup>24</sup>S. V. Polyakov and A. L. Migdall, *J. Mod. Opt.* **56**, 1045 (2009).
- <sup>25</sup>J. Lavoie, J. M. Donohue, L. G. Wright, A. Fedrizzi, and K. J. Resch, *Nat. Photonics* **7**, 363 (2013).
- <sup>26</sup>M. Allgaier, V. Ansari, L. Sansoni, C. Eigner, V. Quiring, R. Ricken, G. Harder, B. Brecht, and C. Silberhorn, *Nat. Commun.* **8**, 14288 (2017).
- <sup>27</sup>L. W. Turner, *Electronics Engineer's Reference Book*, 4th ed. (Butterworth-Heinemann, London, Boston, 1976).
- <sup>28</sup>A. Secroun, A. Mens, D. Gontier, P. Brunel, J.-C. Rebuffie, and C. Goulmy, *Proc. SPIE* **3429**, 32–38 (1998).
- <sup>29</sup>L. M. Davis and C. Parigger, *Meas. Sci. Technol.* **3**, 85 (1992).
- <sup>30</sup>O. H. W. Siegmund, J. Vallergera, and B. Wargelin, *IEEE Trans. Nucl. Sci.* **35**, 524 (1988).
- <sup>31</sup>HAMAMATSU PHOTONICS K.K., Systems Division, “Universal Streak Camera C5680 Series,” (2003).
- <sup>32</sup>HAMAMATSU PHOTONICS K.K., Systems Division, “NIR Streak Camera C11293-02,” (2015).
- <sup>33</sup>G. Harder, V. Ansari, B. Brecht, T. Dirmeier, C. Marquardt, and C. Silberhorn, *Opt. Express* **21**, 13975 (2013).
- <sup>34</sup>A. Eckstein, B. Brecht, and C. Silberhorn, *Opt. Express* **19**, 13770 (2011).
- <sup>35</sup>B. Brecht, A. Eckstein, R. Ricken, V. Quiring, H. Suche, L. Sansoni, and C. Silberhorn, *Phys. Rev. A* **90**, 030302 (2014).
- <sup>36</sup>V. Ansari, G. Harder, M. Allgaier, B. Brecht, and C. Silberhorn, *Phys. Rev. A* **96**, 063817 (2017).
- <sup>37</sup>B. Brecht, A. Eckstein, A. Christ, H. Suche, and C. Silberhorn, *New J. Phys.* **13**, 065029 (2011).
- <sup>38</sup>A. P. Baronavski, H. D. Ladouceur, and J. K. Shaw, *IEEE J. Quantum Electron.* **29**, 580 (1993).
- <sup>39</sup>M. G. Raymer, D. V. Reddy, S. J. van Enk, and C. J. McKinstrie, preprint [arXiv:1710.07159](https://arxiv.org/abs/1710.07159) (2017).